Hybrid Channel Codes for Efficient FSO/RF Communication Systems

Ali Eslami, *Student Member, IEEE,* Sarma Vangala, *Student Member, IEEE,* and Hossein Pishro-Nik, *Member, IEEE*

***Abstract*—Conventional hybrid RF and optical wireless communication systems make use of parallel Free Space Optical (FSO) and Radio Frequency (RF) channels to achieve higher reliability than individual channels. True hybridization can be accomplished when both channels collaboratively compensate the shortcomings of each other and thereby improve the performance of the system as a whole. In this paper, we propose a novel coding paradigm called "Hybrid Channel Coding" that not only optimally achieves the capacity of the combined FSO and RF channels but also can potentially provide carrier grade reliability (99.999%) for hybrid FSO/RF systems. The proposed mechanism uses non-uniform and rate-compatible LDPC codes to achieve the desired reliability and capacity limits. We propose a design methodology for constructing these Hybrid Channel Codes. Using analysis and simulation, we show that by using Hybrid Channel Codes, we can obtain significantly better availability results in terms of the required link margin while the average throughput obtained is more than 33% better than the currently existing systems. Also by avoiding data duplication, we preserve to a great extent the crucial security benefits of FSO communications. Simulations also show that Hybrid Channel Codes can achieve more than two orders of magnitude improvement in bit error rate compared to present systems.**

***Index Terms*—LDPC codes, rate-compatible codes, non-uniform codes, FSO/RF hybrid system.**

I. Introduction

FREE Space Optical (FSO) communication systems, also known as wireless optical communications, provide tremendous potential for low-cost time-constrained high-bandwidth connectivity in a variety of network scenarios. Several long-standing problems such as last mile connectivity, broadband internet access to rural areas, disaster recovery and many others can be solved using FSO communication systems. This is because, point-to-point line-of sight (LOS) FSO communication systems can achieve data rates comparable to fiber optics without incurring exorbitant costs and requiring significant amount of time for installation. However, the widespread deployment of FSO communication systems has been hampered by the reliability or availability issues related to atmospheric variations [1], [2]. FSO communication undergoes significant deterioration whenever the visibility in the medium is affected especially in cases of smoke and fog. In general, the atmospheric effects on the laser beam propagation can be broken down into two categories: attenuation of the laser power and fluctuations of the laser power due to the laser beam deformation, called "atmospheric turbulence" [3]–[9]. Atmospheric turbulence and its effect on the FSO Channel has been studied in many papers [10]–[20] and many effective ways to combat turbulence-induced fading are proposed in the literature like special coding techniques, interleaving, and different diversity schemes. While the contribution of atmospheric turbulence is comparatively small, attenuation is the most critical factor for longer FSO links [3]–[9]. The main cause of the attenuation is the impact of the weather condition; even a modest fog can cause 40 dB/km attenuation and a medium rain of 12.5 mm/hr can lead to 4.6 dB/km loss. In fact, system outages due to extreme weather conditions can make the link completely useless or reduce the range of transmission [3]–[9]. In such situations, along with error control codes, range reduction using multiple hops can be used to increase channel availability [21]. However, this can lead to an increase in the expenditure on equipment and inefficient utilization of the system whenever the channel conditions become normal again.

Because of all these issues, the idea of media or channel diversity [5], [8], [22] emerged to improve channel utilization without any of the negative effects of interleaving or range reduction. In this diversity scheme, which is the basis for hybrid FSO/RF communications, a complementary RF link is utilized to back up the FSO link [5], [8], [22]. In [22], the authors propose the use of a low-capacity RF channel which is used only when the optical wireless channel is down. Another system makes use of a 60GHz MMW channel in conjunction with the FSO channel [22], [23]. There are two reasons for such a combination. First, using MMW data transmission allows the RF link to achieve data rates comparable to that of the FSO link, i.e. over 1 Gbps. Second, the two channels provide an optimum combination for high availability since MMW communication is mostly affected by rain and snow while FSO communication suffers most in fog [5], [8], [22], [23]. Redundancy in transmission over two disparately-behaving channels probabilistically improves the chance of message recovery at the receiver and provides viable solutions to the availability problem. It is shown that hybrid FSO/RF communication systems achieve carrier-class availability of

Paper approved by K. Kitayama, the Editor for Photonic Networks and Fiber Optic Wireless of the IEEE Communications Society. Manuscript received April 12, 2009; revised September 28, 2009 and February 23, 2010.

The material in this paper was presented in part at the 41st IEEE Annual Conference on Information Sciences and Systems, 2007, and the IEEE Global Telecommunications Conference, 2007. This work was supported by the National Science Foundation under grants ECCS-0636569 and CCF-0830614.

The authors are with the Department of Electrical and Computer Engineering, University of Massachusetts, Amherst, MA 01003 USA (e-mail: {eslami, svangala, pishro}@ecs.umass.edu).

Digital Object Identifier 10.1110/TCOMM.2010.082710.090195

99.999% [5], [8], [22], [23]. Error control coding schemes can be used in these scenarios as well where media diversity helps mitigate the long term bursts and the error control coding helps reduce the bit error rates. However, the current approach to hybrid FSO/RF communication is inefficient and suffers from certain inherent problems. In some of the current hybrid systems, the RF transmitter remains silent when the FSO link is working normally and in others, it only duplicates the data sent on the FSO link. Both schemes lead to the wastage of bandwidth and under-utilization of the RF link. Furthermore, FSO communication is inherently secure because disruption of the link needs a direct obstruction of the point-to-point link. However, retransmission of the message over the insecure RF channel leads to an insecure communication system. Also, frequent switching between the FSO and RF links, called flapping [24], can lead to a collapse of the communication system. This undesirable behavior arises if the FSO and RF links become alternately unavailable for short periods of time. Moreover, the need for multiple encoders and decoders results in increased costs and synchronization issues. In this paper, we introduce a new coding paradigm called "Hybrid Channel Coding" that utilizes both channels to the fullest extent and still makes hybrid FSO/RF communication systems achieve carrier-class reliability. "Hybrid Channel Codes" combine non-uniform codes and rate-adaptive codes using only a single encoder and decoder to vary the code-rate based on the channel conditions. Media diversity in combination with non-uniform codes is used to overcome long channel outages and rate-adaptivity is used to always provide a throughput near the capacity of our time-varying channel [25]. Additionally, the non-uniform codes used are of long block lengths that allow utilization of LDPC codes to their fullest potential. True hybridization can be accomplished when both channels collaboratively compensate the shortcomings of each other and thereby, improve the performance of the system as a whole in terms of availability, bit error rate, effective channel throughput, and information security.

The rest of this paper is organized as follows. In Section II, we will introduce and analyze Hybrid Channel Coding which is the main idea of this paper. This section will provide the theoretical basis of the paper. In Section III, we give a comparison of existing systems with our proposed system in terms of system availability and average throughput obtained and show that the proposed scheme can lead to significant performance improvements. Section IV provides simulation results to support our claims and Section V concludes the paper.

II. Hybrid Channel Codes

The hybrid FSO/RF channel consists of two communication channels both of which are time-variant. In order to achieve efficient and reliable communication on the hybrid FSO/RF link we propose a novel coding paradigm, called *Hybrid Channel Codes*. This coding scheme is based on two important concepts: non-uniform (multi-channel) coding, and rate-compatible (rate-adaptive) coding. Non-uniform codes were recently proposed in [26]. They provide a highly efficient and reliable communication scheme over several parallel channels using modern codes such as low-density parity-check (LDPC) codes. However, these codes are designed for the scenarios in which the channels are fixed, i.e. time-invariant. Rate-compatible LDPC codes have been shown to achieve close-to-capacity performance for highly time-variant channels using only one encoder and decoder [27], [28]. The main idea behind Hybrid Channel Codes is to combine non-uniform coding and rate-adaptive coding using LDPC codes. An LDPC code is defined by a sparse parity-check matrix $H = [h_{ij}]$. LDPC codes can be represented by their Tanner graphs [29]. The Tanner graph is a bipartite graph with two sets of nodes, the variable nodes and the check nodes. The variable nodes denote the codeword bits and the check nodes denote the parity check equations satisfied by the codeword bits. A check node c_i is connected to a variable node v_j whenever $h_{ij} = 1$. Fig. 1 shows a parity check matrix and the corresponding Tanner graph. The degree of a node is equal to the number of edges that are connected to that node. The degree distribution for random LDPC codes is usually represented by a polynomial pair (λ, ρ) [30] where $\lambda(x) := \sum_{i=2}^{d_v} \lambda_i x^{i-1}$ ($\rho(x) := \sum_{i=2}^{d_c} \rho_i x^{i-1}$) specifies the variable (check) node degree distribution. More precisely, λ_i (ρ_i) represents the fraction of edges emanating from variable (check) nodes of degree i. The maximum variable degree and check degree is denoted by d_v and d_c, respectively. LDPC codes can be efficiently decoded by a suboptimal iterative algorithm called *message passing*. In this method, at first the log-likelihood ratios (LLRs) for channel outputs are calculated at variable node. Then every variable node passes its calculated LLR to all adjacent check nodes on the Tanner graph. Every check node then updates the LLR value for each of its adjacent variable nodes and sends it as a response. The updated value of LLR for each variable node is calculated using the LLRs provided to the check node by other adjacent variable nodes. In the next step, every variable node updates its LLR using the messages received by its adjacent check nodes, and then sends it back to them. The last two steps are repeated at the decoder until either the codeword is decoded correctly or a pre-determined iteration number is reached. The messages passed between the variable and check nodes are shown in Fig. 1 by $m_{v_j c_i}$ and $m_{c_i v_j}$.

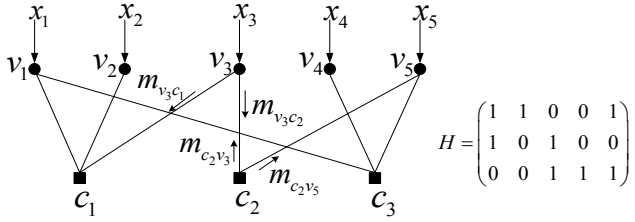

Fig. 1. Tanner graph representation of LDPC codes and message passing algorithm for decoding.

Fig. 2 depicts the structure of Hybrid Channel Codes using LDPC codes. In this paper, we consider the construction of rate-compatible LDPC codes via puncturing, one of the most common methods used to construct rate-compatible codes. In this method, in order to change the rate of a code to a higher rate, we puncture (delete) a subset of the codeword

bits [26], [27]. In fact, punctured codes use the same encoder and decoder for all rates. Let $\Re = \{r_1, r_2, ..., r_s\}$ be the set of different rates that are needed. Let r_p be the rate of the parent code (i.e. the lowest rate in $\Re$). One can design an optimized LDPC code of rate $r_p = \frac{k}{n}$ where k and n are the lengths of information blocks and the codewords, respectively. To guarantee a code with a new rate, we find an optimum puncturing of a subset of bits in the codeword and send the punctured codeword to the receiver. Note that the punctured bits will not be transmitted as is shown in Fig. 2. The set of positions of punctured bits for a desired rate is called the *puncturing pattern* for that rate. Puncturing patterns for all the rates in $\Re$ are known by the decoder due to an off-line setup. In Fig. 2, $v_1, v_2, ..., v_n$ represent the outputs of parent encoder with rate $\frac{k}{n}$. The code which is used here is a non-uniform code (will be described later). The coded bits are of two types; they are either a FSO bit or a RF bit. That is they are going to be sent over either the FSO channel or RF channel. It is assumed that both channel states information are available at the transmitter so that the appropriate puncturing pattern can be chosen for the set of bits of each type. In the figure, we have shown an example of the puncturing pattern in which "P" denotes the position of punctured (deleted) bits and the position of preserved bits are shown by "$\rightarrow$". The percentage of punctured bits determines the code rate for each type. The resulted blocks are sent over the channels. At the beginning of the iterative decoding, the log-likelihood ratios (LLRs) for the punctured bits are set to zero. It is shown that punctured LDPC codes exhibit desirable properties [31]. First, the performance of a good LDPC code is maintained for a wide rage of rates. Second, there is no theoretical limitation on the number of rates or the values of rates we can generate. It is also shown that random punctured LDPC codes usually have good performance [26], [27].

In a hybrid FSO/RF system, our goal is to transmit data bits over two parallel channels, i.e. FSO and RF channels. One trivial approach is to design a separate error-correcting code for each channel. Here, however, we are interested in designing only one LDPC code as shown in Fig. 2. Suppose we use a code of length n. We transmit any codeword over the two channels such that n_1 bits are transmitted over the FSO channel and n_2 bits in any codeword are transmitted over the RF channel, so $n = n_1 + n_2$. As a simple example, consider the tanner graph of Fig. 1 and assume that we are sending degree 2 variable bits, i.e. v_1, v_3, v_5, on the FSO channel and degree one variable bits, i.e. v_2, v_4, on the RF channel. In [26], it is shown that for certain practical problems, this approach, called non-uniform coding, provides advantages over using separate encoders. We use the Tanner graph representation to define the ensemble $g(\Lambda, \rho)$ of bipartite graphs for non-uniform FSO/RF channels. Let E be the set of edges in the graph and let E^{RF} and E^{FSO} be the set of edges that are incident with variable nodes corresponding to the RF and FSO channels, respectively. Also let E_i^{RF} be the set of the edges that are adjacent to the RF variable nodes of degree i. We define $\lambda^{RF}(x) = \sum \lambda_i^{RF} x^{i-1}$ where $\lambda_i^{RF} = \frac{|E_i^{RF}|}{|E^{RF}|}$. Also, define $\lambda^{FSO}(x)$ accordingly. Let $\Lambda = \{\lambda^{FSO}(x), \lambda^{RF}(x)\}$ and $\rho(x) = \sum \rho_i x^{i-1}$, where ρ_i is the fraction of edges connected to a check node of degree i [30]. The ensemble is defined as the ensemble of bipartite graphs with degree distributions given by Λ and ρ. In other words, in the ensemble $g(\Lambda, \rho)$, variable nodes corresponding to bits of different channels have different degree distributions. In fact, the code is designed with the prior knowledge of which bits are transmitted over each channel. The important fact about the ensemble $g(\Lambda, \rho)$ is that unlike ordinary ensembles of LDPC codes, we can use this information in the code design. This extra information results in several advantages of the ensemble $g(\Lambda, \rho)$ over the ordinary ensembles. Note that ensemble $g(\Lambda, \rho)$ is a generalization of the ordinary ensembles of LDPC codes. In fact, by choosing $\lambda^{FSO}(x)$ and $\lambda^{RF}(x)$ equivalent we obtain an ordinary ensemble of LDPC codes. Thus, in all circumstances, the performance of the non-uniform codes is at least as good as the ordinary ensembles. This comes with even simpler design of these codes. In fact, in ordinary LDPC codes in order to approach channel capacity we need to use highly irregular codes. However, in non-uniform codes part of the required irregularity is achieved by channel nonuniformity. This will simplify the degree optimization significantly. Another important advantage is that we can benefit our extra information in code design to use lower values for variables in the degree distribution. This means that we can obtain sparser codes which in turn results in faster decoding and more efficient implementation [26].

Throughout the paper, we assume that the number of RF punctured nodes is given by np_{RF}, where p_{RF} is the fraction of RF nodes that are punctured. Similarly, the number of FSO punctured nodes is given by np_{FSO}. We also define, $\phi = \frac{np_{RF}}{n_{RF}}$ and $\psi = \frac{np_{FSO}}{n_{FSO}}$. Given the already established advantages of rate-adaptive and non-uniform coding, Hybrid Channel Coding is a very promising scheme. In the following sections, we provide analysis and design of these codes for efficient and reliable communication. In particular, we first show that Hybrid Channel Codes are capacity-achieving under maximum likelihood decoding. We then provide density evolution analysis to show their performance under iterative decoding and then provide the design of optimal Hybrid Channel Codes. We obtain the achievable rate regions for iterative decoding. Using the simulation results, we confirm that these codes provide efficient and reliable communication over hybrid FSO/RF channels. It should be mentioned that in our analytic results, we have assumed the two channels to be memoryless to keep the math manageable.

A. Optimality of Hybrid Channel Codes for Hybrid FSO/RF Channels

Here we state a fundamental result asserting that Hybrid Channel Codes are essentially optimal for hybrid FSO/RF systems. The optimality of these codes combined with other advantages described above, makes them an ideal candidate for hybrid FSO/RF channels. Consider two independent channels C_1 and C_2 that are used in parallel. Suppose c_1 and c_2 are the capacities of the two channels respectively. Since the channels are independent, from an information theoretic point of view, the maximum achievable data rate using this system is $r_{max} = \frac{c_1 + c_2}{2}$. Note that we normalized the capacity to remain less than one. In our specific case of time-variant FSO/RF

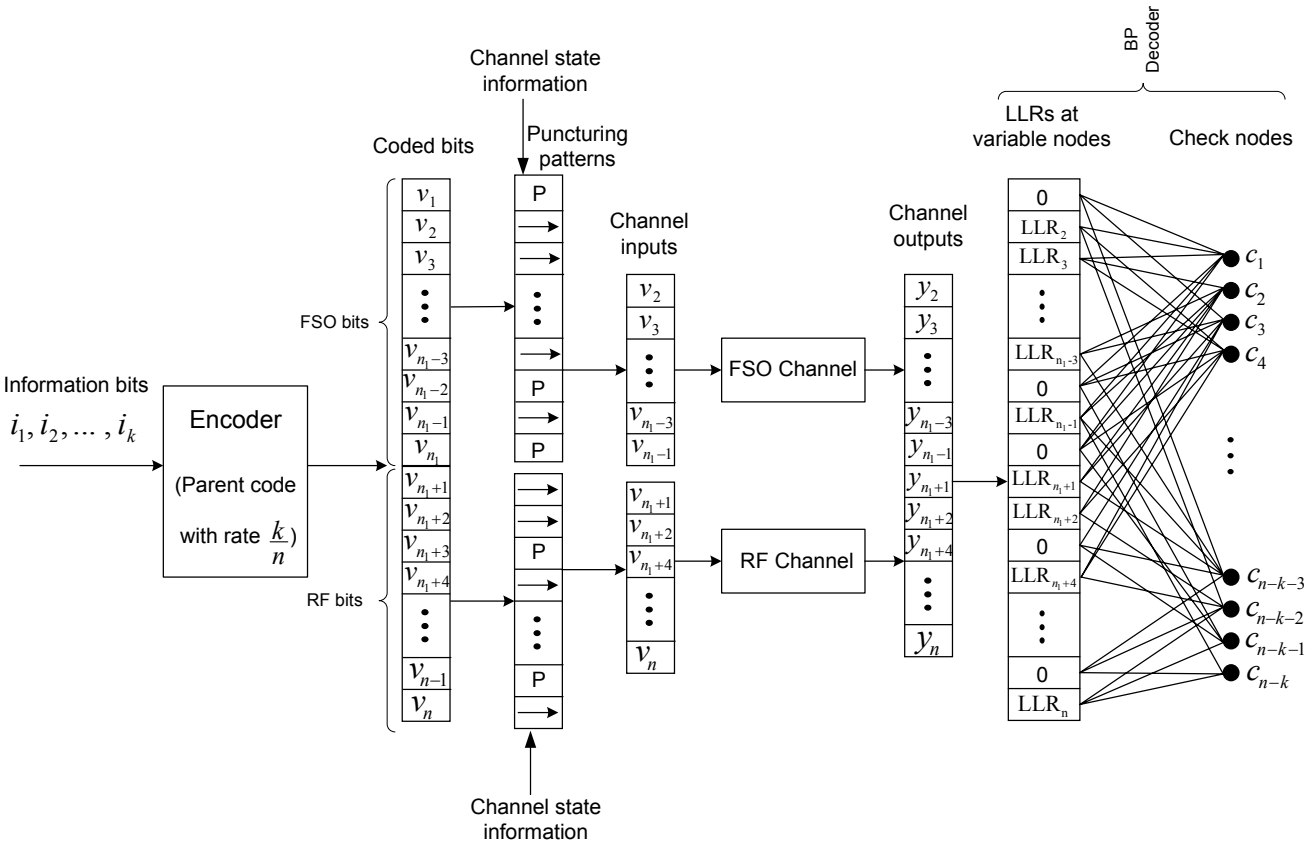

Fig. 2. Graphical representation of Hybrid Channel Codes. In the figure, it is assumed that n_1 bits of n coded bits are FSO bits and $n - n_1$ bits are RF bits.

channels, c_1 and c_2 change over time and so does r_{max}. The main idea behind Hybrid Channel Coding is to achieve the data rate $r_{max} = \frac{c_1+c_2}{2}$, independent of the channel conditions. That is, we want to achieve the highest possible data rate at any time. Clearly, no scheme can achieve higher rates than the mentioned scheme, since this limit is imposed by information theory. We now state a result saying that Hybrid Channel Codes can achieve r_{max} at all times. This important result implies that only one encoder and decoder can be used to achieve the capacity of a time-variant hybrid channel. Note that, we have proved the result for maximum likelihood decoding. In practice, we use simple iterative decoding which has been shown, by simulation, to perform very close to maximum likelihood decoding for optimal codes.

Theorem 1: Let C_1 and C_2 be two binary-input output-symmetric memory-less (BIOSM) channels, that are used in parallel. Let α and β be two fixed real numbers in (0,1). Assume the capacities of C_1 and C_2 at any time t is given by $c_1(t)$ and $c_2(t)$, where $\alpha < c_1(t), c_2(t) < \beta$. For any $\epsilon > 0$, there exists a Hybrid Channel Code that achieves the rate $r_{max}(t) = \frac{[c_1(t)+c_2(t)]}{2}(1-\epsilon)$ at all times. This is done by proper puncturing and using maximum likelihood decoding at the receiver.

Proof: The theorem can be proved using conventional information theoretic proofs, however, we find the following proof interesting and short. Consider the case where the channel capacities are the minimum in the range we are studying. That is assume $c_1(t) = c_1^{min} \geq \alpha$, and $c_2(t) = c_2^{min} \geq \alpha$. Let $R_0 = \frac{c_1^{min}+c_2^{min}}{2}(1-\epsilon)$. Note that here we assume the code rates and channel capacities are always between 0 and 1. Thus, capacity achieving codes have rates close to $\frac{c_1^{min}+c_2^{min}}{2}$. We construct an ensemble of LDPC codes suggested by MacKay [32], in which columns are constructed independently and randomly and they have weight t. The code rate is chosen to be R_0. This code will be our parent code. As it is proved in [33], the ensemble can achieve the capacity of BIOSM channels. Thus for sufficiently large t, the error probability for any BIOSM channel with capacity smaller than R_0 can be made arbitrarily small.

Now assume that the channel conditions improve, and the capacities become c_1 and c_2 respectively. Let the puncturing fraction, p, be chosen as

$$p = 1 - \frac{c_1^{min} + c_2^{min}}{c_1 + c_2}.$$

The punctured bits are chosen randomly from the codeword bits. This doesn't mean that we pick a random puncturing pattern for every block. In fact, for each code rate, a random pattern will be chosen and implemented in the code design stage. The interesting point is that this system can be modeled as the system shown in Fig. 3 [26]. In this figure, the puncturing effect is modeled by two binary erasure channels (BECs) with erasure probabilities p. Note that the output of the erasure channels in this model is not ternary. In fact, the decoder is aware of the positions of the punctured (erased)

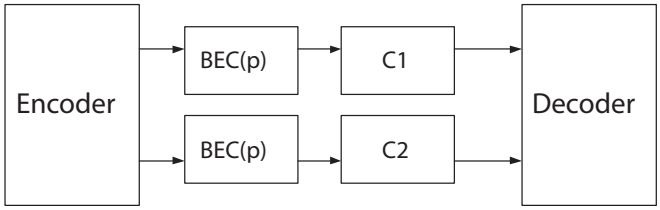

Fig. 3. Proof of Theorem 1.

bits and sets their initial LLRs to zero for decoding. As it is shown in [33], the error rate is vanishing as long as the code rate is smaller than the capacity of the channel. The equivalent channel has the capacity:

$$c_{eq} = \frac{1}{2}[c_1(1-p) + c_2(1-p)] = \frac{1}{2}(c_1^{min} + c_2^{min}).$$

Thus the error probability goes to zero as t goes to infinity. But the code rate of the punctured code is given by

$$R = \frac{R_0}{1-p} = \frac{c_1 + c_2}{2}(1-\epsilon).$$

Thus we conclude all rates smaller than $\frac{c_1+c_2}{2}$ are achievable. Therefore, we can achieve the channel capacity at all times. It should be mentioned that we can also prove this theorem using a similar method to [34]. ■

This important result assures us that from a theoretical point of view, Hybrid Channel Codes are suitable for the hybrid FSO/RF systems. Interestingly, the Hybrid Channel Codes achieve optimal rates deploying only one encoder and decoder. For example, even if one of the channels completely fails, i.e. the signal-to-noise ratio drops drastically, we still have reliable communications as long as the other channel has a good signal-to-noise ratio. In this case, we can simply shut off the corresponding transmitter without manipulating the encoder and the decoder. In fact, the decoder assumes that the unused channel has zero capacity. This versatility of the coding scheme is a significant advantage over existing FSO/RF systems, since it avoids any problematic issues of switching between the two channels.

Note that the theorem assumes both channels to be memoryless. This assumption is used to simplify the analysis, though it is not always true. In fact, the scattering experienced by laser beam in an optically thick medium, such as a heavy fog, introduces memory to the FSO channel [35]–[37]. This memory sets an upper bound on the achievable communication rate. Although this memory can be made small by choosing a small field of view in the receiver, it cannot be totally removed in practice [37]. Several methods have been proposed in the literature to address the Inter-Symbol Interference (ISI) caused by the channel memory [38], [39]. A well-studied method is to use a multi-carrier scheme such as Orthogonal Frequency-Division Multiplexing (OFDM) for signal transmission [38], [40]. OFDM splits a high-data rate data-stream into a number of low-rate data-streams that are transmitted simultaneously over a number of sub-carriers. This way, the aggregate data rate can be divided among many sub-carriers, and since per channel OFDM symbol rate is much lower, the intrachannel nonlinearities can be completely avoided [38]. Along with OFDM, one can also use equalization to mitigate the ISI, benefiting from the fact that employing OFDM makes it easier to implement equalizers for the resulted narrow-band sub-channels [39]. In Section IV, we will show how OFDM can be exploited along with Hybrid Channel Codes to make a robust hybrid FSO/RF system in different channel conditions.

Furthermore, it should be noted that in the case of a heavy fog or cloud, the FSO channel loses most of its capacity, making the RF link to take the burden of transmitting the main portion of data. In this case, Hybrid Channel Codes achieve the capacity of RF channel which is in fact a big portion of the combined channel capacity. As a result, our proposed scheme would be able to perform close to capacity despite the memory that can be introduced to the FSO channel in an optically thick medium.

It is worth noting that the capacity of the combined channels can also be achieved by using two separate encoders, each being capacity achieving for the corresponding channel. However, the main issue here is that, the proposed hybrid codes have several important advantages over the separate-codes method including:

- providing higher availability
- benefitting from all advantages of using non-uniform coding
- lower complexity resulted by using only one encoder-decoder.

We will explain these advantages in Section III-B where we discuss the performance characteristics of different systems including the one with separate capacity achieving encoders.

B. Density Evolution

Here, we provide density evolution formulas to analyze the performance of Hybrid Channel Codes under iterative decoding. Assume that the RF and the FSO channels are memory-less binary-input output-symmetric (MBIOS) channels. Let γ_{RF} and γ_{FSO} be the signal to noise ratios (SNR) of the RF and FSO channels respectively. The SNRs show the channel conditions and depend on the signal intensity and the noise level. We assume that γ_{RF} and γ_{FSO} are real numbers in $[0, +\infty]$. Thus $\gamma = +\infty$ refers to the perfect channel conditions and $\gamma = 0$ refers to the case where the channel capacity is zero. For the RF channel, assuming that all-one code word has been sent, we define the random variable $Z_{\gamma_{RF}}$ as the log likelihood ratio of the transmitted bits, given that the SNR is γ_{RF}. Let $F_{RF}(z, \gamma_{RF})$ and $f_{RF}(z, \gamma_{RF})$ be the cumulative distribution function (CDF) and the probability density function (PDF) of $Z_{\gamma_{RF}}$ respectively. Similarly, define $Z_{\gamma_{FSO}}$, $F_{FSO}(z, \gamma_{FSO})$ and $f_{FSO}(z, \gamma_{FSO})$.

Recall the setting we described above for the ensemble $g(\Lambda, \rho)$ of non-uniform codes. Similar to [30], we can find the density evolution formulas for the Hybrid Channel Codes ensemble. Let us define $q^{RF} = \frac{|E^{RF}|}{|E|}$ and $q^{FSO} = \frac{|E^{FSO}|}{|E|}$. Let P_l^{RF} denote the probability density function of the messages that are sent from RF variable nodes in the lth iteration of the message passing decoding. Define P_l^{FSO} accordingly. Then, the formulas for density evolution can be written as

$$P_0^{RF}(x) = \phi\delta(x) + (1-\phi) f_{RF}(x, \gamma_{RF}),$$
$$P_0^{FSO}(x) = \psi\delta(x) + (1-\psi) f_{FSO}(x, \gamma_{FSO}),$$

$$P_l^{RF} = P_0^{RF} \otimes \lambda^{RF}\left(\Gamma^{-1}\left[\rho(\Gamma(q^{RF}P_{l-1}^{RF} + q^{FSO}P_{l-1}^{FSO}))\right]\right),$$

$$P_l^{FSO} = P_0^{FSO} \otimes \lambda^{FSO}\left(\Gamma^{-1}\left[\rho(\Gamma(q^{RF}P_{l-1}^{RF} + q^{FSO}P_{l-1}^{FSO}))\right]\right),$$

where $\otimes$ denotes convolution and Γ is as defined in [30]. These results are obtained by applying the density evolution analysis of non-uniform codes [26], and punctured codes [27] to the Hybrid Channel Code ensemble. We can use these formulas to optimally design Hybrid Channel Codes. The simulation result will confirm the effectiveness of the design methodology.

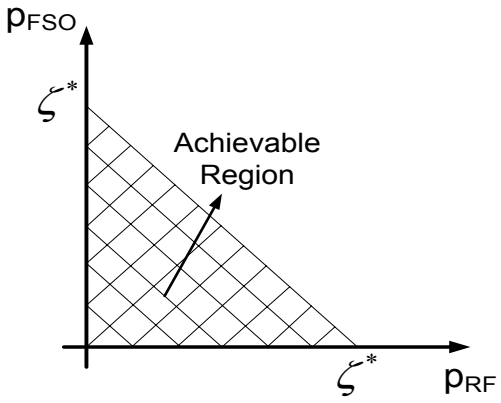

Fig. 4. The achievable region for the puncturing pair $[p_{RF}, p_{FSO}]$.

C. Achievable Rate Region for Iterative Decoding

Here we provide achievable regions for Hybrid Channel Codes. In other words, we provide an exact characterization of the achievable puncturing patterns for a given Hybrid Channel Code ensemble. This is very useful because we can determine the achievable rates and these can be used in the design of efficient codes. We say that a puncturing pair $[p_{RF}, p_{FSO}]$ is achievable for an ensemble of Hybrid Channel Codes if there exist $\gamma_{RF} < +\infty$ and $\gamma_{FSO} < +\infty$ such that a randomly chosen code from the ensemble can be used to achieve arbitrarily small error rate over the hybrid FSO/RF channel with SNRs γ_{RF} and γ_{FSO}. Otherwise, the pair $[p_{RF}, p_{FSO}]$ is not achievable.

Theorem 2: For an ensemble of Hybrid Channel Codes, define $x_0(\zeta) = 1$, and $x_l(\zeta) = \lambda\big(1 - \rho(1 - \zeta x_{l-1})\big)$, for $l = 1, 2, \ldots$. Let ζ^* be the maximum value for which $\lim_{l\to\infty} x_l(\zeta^*) = 0$. The puncturing pair $[p_{RF}, p_{FSO}]$ is achievable if and only if $p_{RF} + p_{FSO} < \zeta^*$.

Proof: Assume $p_{RF} + p_{FSO} > \zeta^*$. Define $y_0(\zeta) = 1$, and $y_l(\zeta) = \lambda\big(1 - \rho(1 - (p_{RF} + p_{FSO})y_{l-1})\big)$. Then $y_l(\zeta)$ is the fraction of erasure messages in the l^{th} iteration from the punctured variable nodes, assuming the noise levels of the channels are both zero. Then, we have $\lim_{l\to\infty} y_l > 0$. This means, even if the noise levels of the RF and FSO channels are zero, the punctured bits are not recovered at the decoder. Thus, the pair $[p_{RF}, p_{FSO}]$ is not achievable.

Now assume $p_{RF}+p_{FSO} < \zeta^*$ and let P_e^l be the probability of error after the l_{th} iteration. Then, using a similar argument as in [27], we can show that there exist $\gamma_{RF_1}, \gamma_{FSO_1} < \infty$ such that if $\gamma_{RF} > \gamma_{RF_1}$ and $\gamma_{FSO} > \gamma_{FSO_1}$, then the punctured ensemble satisfies the stability condition. By stability condition, there exists a constant $\delta > 0$ such that if $P_e^l < \delta$ for some $l \in \mathbb{N}$, then P_e^l converges to zero as l tends to infinity. However, $x_l(\zeta)$ is a continuous function of ζ. Thus, by the conditions of the theorem, for any $\epsilon > 0$ there exists a $l_1 \in \mathbb{N}$ such that for $l > l_1$ we have $x_l(\zeta) < \epsilon$. Now, let $\epsilon = \delta$. Thus, for every $\gamma_{RF} > \gamma_{RF_1}$ and $\gamma_{FSO} > \gamma_{FSO_1}$, the stability condition is satisfied and P_e^l converges to zero as l goes to infinity. ∎

The achievable region for Hybrid Channel Codes is shown in Fig. 4. It is noteworthy that our theorems on Hybrid Channel Codes are independent of the channel model. In fact, we can expect that carefully designed Hybrid Channel Codes exhibit near-capacity performance when the channel is either dominated by fading or by attenuation. However, FSO and RF channels in hybrid FSO/RF systems have their own specific models which we explain in detail in next section and use to run our simulations.

III. Performance Comparison for Different FSO/RF Systems

In this section, we give a brief comparison of the performance of our proposed scheme using Hybrid Channel Codes with currently existing systems. First, we present the channel model which we will use for FSO and RF channels.

A. Channel Model

The channel model defined here is similar to the one used in [5]. The FSO and RF channels can be modeled as

$$\begin{aligned} Y_1 &= A_1 h_1 X_1 + N_1, \quad A_1, h_1 > 0, \\ Y_2 &= A_2 h_2 X_2 + N_2, \quad A_2, h_2 > 0, \end{aligned} \tag{1}$$

where X_1 and X_2 denote, respectively, the transmitted binary signals over FSO and RF channel, A_1 and A_2 denote the channel attenuations, h_1 and h_2 denote the fading gains, and $N_1 \sim \mathcal{N}(0, \sigma_{N_1}^2)$ and $N_2 \sim \mathcal{N}(0, \sigma_{N_2}^2)$ are independent gaussian random variables representing the noise. The values of channel attenuations A_1 and A_2 depend on the weather condition.

There are several formulae used in the literature to model the FSO and RF channels under different channel conditions and for different atmospheric phenomena like fog, rain and snow [3]–[9]. We adopt the model described in [5] and in fact, we only consider the effect of fog and rain for FSO channel and the rain for RF channel as they are the main causes of outage in each of these channels [3]–[9]. We assume a working wavelength of $1550\ nm$ for our FSO transmitter. In order to model the attenuation due to fog, we use the Kim model [41] which is one of the most widely used models and allows to calculate the attenuation based on the visibility data. The attenuation of fog can be represented by

$$A = e^{\sigma_{fog} L},$$

where σ_{fog} is the attenuation coefficient and L is the link distance which we assume is 1.5 km for our systems. The relation of visibility and attenuation is given by

$$\sigma_{fog} = \frac{3.91}{V}(\frac{\lambda}{550})^{-q}, \quad (2)$$

where V is the visibility in km, λ is wavelength in nm, and q is the exponent related to particle size distribution given by

$$q = \begin{cases} 1.6 & V > 50km \\ 1.3 & 6km < V < 50km \\ 0.16V + 0.34 & 1km < V < 6km \\ V - 0.5 & 0.5km < V < 1km \\ 0 & V < 0.5km. \end{cases} \quad (3)$$

The rain attenuation for both of the FSO and RF channels can be modeled by the equation

$$\alpha_{rain} = a \times R^b \ [dB/km], \quad (4)$$

where R is the rain rate in mm/hr, and a and b depend on frequency, temperature and the climate region [42]. We assumed a working wavelength of $1550\ nm$ and $5\ mm$ for the FSO and RF transmitters, respectively, which for a raindrop temperature of $0°$C in Boston, MA results in the values of $a_{FSO} = 1$ and $b_{FSO} = 0.66$ for the FSO channel and $a_{RF} = 0.65$ and $b_{RF} = 0.84$ for the RF channel [42].

For the probability density function (pdf) $f_1(h_1)$ of h_1 we adopt the popular Gamma-Gamma fading model [43]

$$f_1(h_1) = \frac{2(\alpha\beta)^{\frac{\alpha+\beta}{2}}}{\Gamma(\alpha)\Gamma(\beta)} h_1^{\frac{(\alpha+\beta)}{2}-1} K_{\alpha-\beta}(2\sqrt{\alpha\beta h_1}),$$

where Γ is the gamma function and $K_{\alpha-\beta}$ is a modified Bessel function of the second kind of order $\alpha-\beta$. Assuming spherical wave propagation, α and β can be directly linked to physical parameters via [43], [44]

$$\alpha = \left[\exp\left(\frac{0.49\chi^2}{(1+0.18d^2+0.56\chi^{12/5})^7/6}\right) - 1\right]^{-1}$$

$$\beta = \left[\exp\left(\frac{0.51\chi^2(1+0.69\chi^{12/5})^{-5/6}}{(1+0.9d^2+0.62d^2\chi^{12/5})^{5/6}}\right) - 1\right]^{-1},$$

where $\chi^2 \triangleq 0.5C_n^2\kappa^{7/6}L^{11/6}$, $d \triangleq (\kappa D^2/4L)^{1/2}$, and $\kappa \triangleq 2\pi/\lambda_1$. Here, λ, D, and C_n^2 are the wavelength, the diameter of the receiver's aperture, and the index of refraction structure parameter, respectively. The fading gain h_2 for the RF channel can also be modeled by Rician K-factor distribution [45], [46].

The scintillation fading process is slow compared to the data rates typical of optical transmission. In fact, the correlation (coherence) time of scintillation is on order of 10^{-2} to 10^{-3} seconds [19], [43]. Thus, in a data rate of many Giga bits per second, millions of consecutive bits may experience nearly identical fading. Given the slow time-varying nature of scintillation, channel state information (CSI) can be estimated at the receiver and fed back to the transmitter via a dedicated feedback link. The transmitter can then adapt the coding rate according to this information. Hence, the idea of rate-adaptive coding seems to suit well this type of channels. The coherence time of fading experienced by the microwave channel is also in order of 10^{-1} to 10^{-2} seconds when the transmitter and receiver are fixed [46], [47]. As a result, we may assume that the values of A_1, A_2, h_1, and h_2 in (1) are known at the transmitter as channel state information. Given the values of these parameters, the two channels can be assumed as independent channels with independent Gaussian noises. This assumption makes the analysis of Section II applicable to our channel model.

B. Performance Comparison of Different Systems

In this section, we compare the performance of different FSO/RF systems in terms of availability and throughput. We define different FSO/RF systems regarding to whether they are using an adaptive or fixed rate coding scheme, and whether they employ a back-up RF channel or not. First, we specify some definitions and assumptions that are used in the rest of the analysis. System availability is usually defined as the percentage of time the intensity of the received signal is above a threshold. To compare different systems, the amount of link margin required for 99.999% availability is usually used.

For a communication system, we define the throughput of the system as the rate of successful message delivery over the communication channel in bits per second. Here, we normalize the throughput to its maximum possible value, i.e. the capacity, and use it as *normalized throughput*. Furthermore, for a system with variable code rate and/or variable capacity, the normalized throughput would be the ratio of the average throughput to the average capacity of the channel, both averaged over the time. We also define the goodput as the ratio of the different data bits (corresponding to the different coded frames), to the capacity of the channel, i.e. from two or more received versions of one frame (e.g. from different channels) we count only one of them in calculating the goodput.

Case 1. Fixed Rate Code on a Single FSO Link: This case can be considered as the base for the rest of the analysis. A system with only the FSO channel and using a fixed rate code has the worst performance (in terms of throughput and channel availability) of all the systems considered. This is due to the lack of any mechanism to compensate for the losses incurred due to the channel variations. The burden of recovering from the channel losses falls completely on the coding mechanism used. Using a high rate code can be detrimental when the coding mechanism is unable to correct all errors. A low rate code would lead to a higher redundancy and bandwidth wastage. This system has been considered in many previous papers. For this system, because even a moderate fog incurs attenuations of more than 40 dB/km, the outage probability stays high even if a margin of 40 dB is implemented. For a typical system of this type and in a typical geographical location, it is shown in [5] that a minimum link margin of 45 dB is needed to obtain the five-nine availability.

Case 2. RF Backup Channel with a Fixed Rate Code: The RF channel can be used as backup in case the FSO link fails. In [5] it is shown that using a back-up RF channel can reduce the required link margins to practical values of 11 dB for FSO and 8 dB for RF channel.

Case 3. RF Backup Channel with Adaptive Codes: The situation can be further improved with an adaptive code which helps increase the channel throughput while the backup RF channel helps increase the system availability. In fact, for

different values of channel attenuation the adaptive code can change its rate to always keep a desired maximum value of bit error rate (BER). Thus we expect the availability to be better than previous cases. For the throughput, note that even though the channel attenuation depends on weather condition and so on the geographical location of the system, most of the time we have a normal weather condition which is clear or relatively clear which leads to low attenuations. Therefore, by using higher code rates for clear channel, we can achieve a significantly better throughput. However, using the RF channel only as a backup like case 2, the system is not efficient in terms of using the available bandwidth of RF channel when the FSO transmitter is active.

Case 4. Independent Parallel FSO/RF Channels with Adaptive Codes: In a system using independent encoders for the FSO and RF channels, data is transmitted over both the FSO and RF channels. In fact, each channel takes responsibility of carrying one portion of the data depending on its capacity. That is, the RF channel is also used for transmitting actual information and does not act only as a backup for the FSO channel. This, in itself, is a novel hybrid FSO/RF approach that can result in a considerable increase in throughput. To the best of our knowledge, no mechanism currently exists that transmits information over both the channels without using the RF channel for repetition or as a backup. In this system, the two channels use separate rate-adaptive codes for each of the FSO and RF links, thus, requiring additional encoder-decoder equipment expenditure. The system availability is equal to that in the case 3. However, the average throughput increases considerably when the RF channel carries actual information . Note that in this system the transmitter is always on and we are using higher average power compared to the cases 2 and 3.

Case 5. Hybrid Channel Codes for Combined FSO/RF Channels: In this system, a single encoder-decoder combination, using Hybrid Channel Codes, is used for the transmission of data. This system is optimized on the sum of the capacities of both the channels combined together (i.e. C_{FSO} + C_{RF}) instead of individual channel capacities C_{FSO} and C_{RF} . Hybrid Channel Codes try to achieve this combined channel capacity. Therefore, benefiting from rate adaptive codes, the average throughput achieved by Hybrid Channel Codes is better than the previously mentioned schemes. This method also utilizes the various advantages that come with non-uniform codes as we discussed in Section II. In this scheme, due to using non-uniform coding, the channel with higher SNR can significantly help the decoding of the other channel. In fact, if only one of the channels is under a low attenuation (which is almost always the case in a hybrid FSO/RF system) we can hope to decode the whole codeword correctly with high probability. The effect of such an interaction between two FSO and RF channels depends on the relative bandwidth of the channels. Usually the bandwidth of the FSO channel is greater than the RF one which makes the FSO channel output a great help to decode the RF channel output correctly. On the other hand, the larger the bandwidth of the RF channel, the more helpful it is for the FSO channel and the performance of Hybrid Channel Codes would be better. Moreover, non-uniform codes allow the usage of long block lengths which result in better error correction properties when used with LDPC codes. Also they provide better error floor performance. So, this scheme is a very good match for FSO/RF systems. After all, simulations show that the Hybrid Channel Coding system needs the least link margin for system availability and yields to the highest throughput of all the FSO/RF systems described.

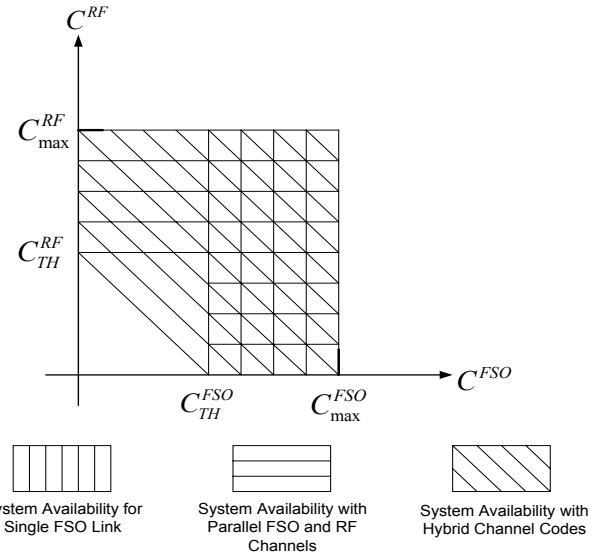

Fig. 5. System availability for different optical wireless systems.

The availability analysis in this section can be represented using Fig. 5. As we mentioned earlier, availability is usually defined as the percentage of time the intensity of the received signal is above a threshold. Equivalently, this can be interpreted as the percentage of time that the capacity of the channel is above a threshold, say C_{TH}. Let's adopt this definition temporarily to explain the availability gain we achieve using Hybrid Channel Codes compared to other approaches. In Fig. 5, the vertically shaded region represents the system availability for Case 1 where there is only a single FSO channel. The system is available whenever the capacity is above the prescribed threshold of the FSO channel. It is clear from the figure that the system availability is increased considerably by using a backup RF channel. This is shown by the horizontally shaded area in the figure. This was discussed earlier in Cases 2, 3. The availability is further increased by using independent parallel encoder-decoders or Hybrid Channel Coding mechanism. This is the cross shaded area in the figure which represents Cases 4 and 5. However, Hybrid Channel Codes use only one encoder-decoder to achieve this capacity region. Also, note that the figure only shows a theoretical overview of the advantages of our proposed systems. The practical implications of using non-uniform codes which allow large block lengths and can provide advantages beyond those shown in the figure are not reflected and will become evident in the simulation results section.

IV. Simulation Results

In this section, we present results confirming our claims presented earlier in the paper. For a system which can adapt

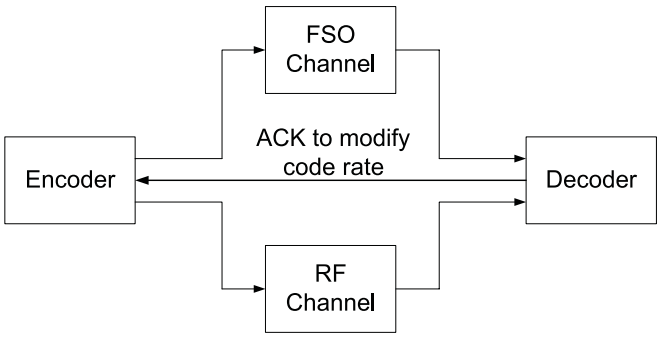

Fig. 6. Simulation setup.

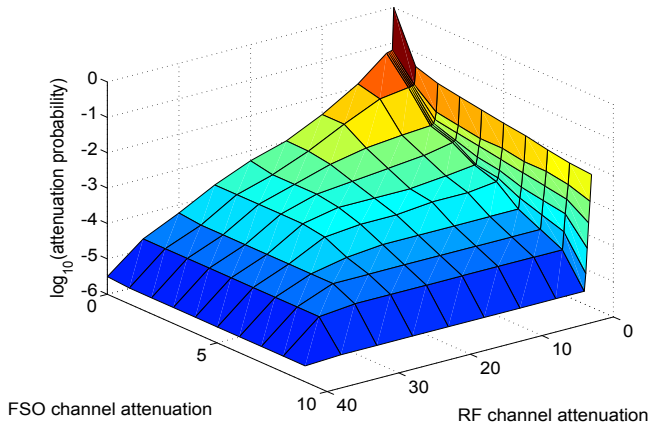

Fig. 7. Attenuation probability of the FSO and RF links based on the measurements of [48].

its code rate based on the channel capacity, we define that the system is available if the bit error rate (BER) is less than a specific value and availability is the percent of time that the system is available. We also use this definition for fixed code rate systems. So, the availability performance of a system is closely related to its BER performance versus signal-to-noise ratio (SNR). However, we provided sufficient discussion on the comparison of different systems' availability in the previous section. In this section, we present the simulation results to observe the effects of Hybrid Channel Codes on channel utilization (or channel throughput) and bit error rate.

A. Simulation Setup

To optimally compare the performance of various coding mechanisms in the varying channel conditions, we use the topology shown in Fig. 6. We assume the existence of separate FSO and RF channels in a parallel topology. Two different systems are considered. In the first system, we assume the FSO channel has a bandwidth of 1 Gbps while the RF channel is assumed to have a bandwidth of 200 Mbps, giving a total channel capacity of 1.2 Gbps. The second system uses an equal bandwidth of 1 Gbps for both the FSO and RF channels [8], [22] and we denote it with equal BW case. In all the simulations, we assume the existence of a retransmission mechanism managed by the upper layers of the system. We consider a feedback channel which is itself subject to error and a limited feedback delay time of 20 code blocks. We assume that the feedback uses a very low code rate (0.15 in our simulations) so that it can be decoded even in bad channel conditions. We also assume that a synchronization mechanism exists at the receiver to combine the data received from both the channels. To run the simulations we need to have the weather information of a specific geographical point, like visibility and rain rate, during a year. We used the measurements of [48] for Boston, Massachusetts. Using (2), (3) and (4), we obtained statistics of the attenuation values experienced by FSO and RF links, shown in Fig. 7. Note that this figure is very similar to Fig. 7 in [5] as it is based on the measurements in a geographically close location to the one considered in [5]. We will use this statistical information when comparing the performance of different systems via simulation.

In order to perform a close-to-realistic simulation, we also need to consider the multipath spread of the signal due to the scattering of laser beam. High densities of small particles distributed in the atmosphere, such as a thick fog, makes the laser beam experience multiple scatterings as it goes through the medium. This phenomenon leads to the temporal dispersion in the received signal, an issue shared by all the FSO systems. The severeness of this multipath spread depends on the optical thickness of the channel [36], [37], [49]; thicker channels suffer from a larger spread of the signal in time. A horizontal link or a link close to the earth, mostly suffers from fog and low-altitude clouds as sources of scattering. A link like the one we assumed of length $1.5\ km$, working in a wavelength of $1.55\ \mu m$, can have an optical thickness of 1 to 50, depending on different weather conditions [36], [37], [49]. These values of the optical thickness, as studied in [36], [37], lead to temporal dispersions on the order of nanoseconds in the collected beam. This implies that a robust system is needed to sustain these values of the temporal dispersion. As we mentioned earlier, some approaches, such as OFDM and equalization, can be used to relax the severe effects of the multipath spread. Here, we employ an OFDM scheme with 128 sub-carriers, resulting in a load of 7.8 Mbps for each sub-channel. This interprets to a symbol time of $128\ ns$ for each sub-channel, assuming BPSK modulation. Now, since the symbol time is much larger than the time spread, the effect of multipath spread is negligible and no equalization is necessary at the receiver. Clearly, one can choose a larger number of sub-carriers if more robustness is required or if severe weather conditions are more likely in the working location of the system. Fig. 8 shows a block diagram of the transmitter and receiver configurations in a system using OFDM. Note that such a configuration is used in the simulation of all the schemes explained in Section III-B. During the simulations, we assumed a worst case time spread of $1\ ns$ for all the schemes.

For the RF channel, we assume that the transmit and receive antenna gains are both 44 dBi and the Rician factor in the channel model is 6[45], [46]. For the parameters in the FSO channel model, we adopt the values used in [44] for the simulations there. We assumed typical aperture diameters of $1\ mm$ and $200\ mm$ for the FSO transmitter and receiver,

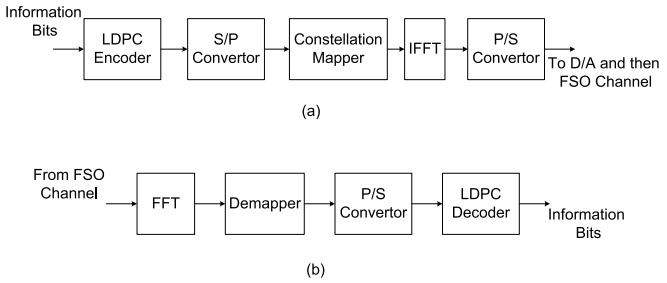

Fig. 8. (a) Transmitter configuration and (b) Receiver configuration using OFDM. S/P–serial to parallel, IFFT–inverse fast Fourier transform, P/S–parallel to serial, D/A–digital to analog, FFT–fast Fourier transform.

respectively. For a single FSO link with a fixed rate code, a fair throughput is obtained in good channel conditions provided the code used is of high rate. However, with a low rate code, the channel utilization is low. After many rounds of simulations we found that the rate 0.7 is somehow optimum for fixed rate scenarios, i.e. the cases 1 and 2 in Section III-B, in the sense that it results in the best throughput providing a reasonable bit error rates (BER) of less than 10^{-6}. A fixed rate code of rate 0.7 and block length $10,000$ was generated using the irregular LDPC code with parameters

$$\lambda(x) = 0.1859\ x^2 + 0.22117\ x^3 + 0.0925\ x^6 + 0.1626\ x^7 + 0.33779\ x^{20},$$

$$\rho(x) = x^{15}.$$

For adaptive scenarios, i.e. cases 3, 4, and 5 in Section III-B, we need to generate a parent code and increase the code rate by puncturing. Considering the analysis of Section II, a code of rate 0.15 was generated as the parent code using the irregular LDPC code with parameters

$$\lambda(x) = 0.4701\ x^2 + 0.1809\ x^3 + 0.1123\ x^5 + 0.0896\ x^6 + 0.1206\ x^{14} + 0.0265\ x^{15},$$

$$\rho(x) = 0.5\ x^3 + 0.5\ x^4.$$

A block length of $10,000$ is chosen for the FSO channel and for the RF channel when it acts only as a back-up, i.e. the cases 2 and 3. For the RF channel, the block length was chosen to be 2000 when using independent parallel encoders with rate adaptive codes. The block length in the case of using Hybrid Channel Codes is the sum of the block lengths on the FSO and RF channels i.e. 12000. This is because we wish to keep the same latency constraints for all the systems being compared. For adaptive coding we use the following rate adaption rule:

$$r = \begin{cases} \frac{i}{10} \quad i = 2, 3, ..., 9 & \text{if} \quad \frac{i}{10} + 0.03 \le c < \min(\frac{i}{10} + 0.13, 1), \\ 0.15 & \text{if} \quad c < 0.23, \end{cases}$$

where r is rate of the code and c is the capacity of corresponding channel. As a non-uniform code, in the case of non-equal BW channels, we send degree 3, 6, 15 and as much as we can of degree 4 variable bits on the FSO channel and the rest of the variable bits on the RF channel. In the equal BW case, we send degree 3, and as much as we can of degree 6 variable bits on the FSO channel and the rest of the variable bits on the RF channel. To find good punctured codes, we calculated the puncturing fractions as discussed in Section II, and then we tried several different random puncturing patterns and finally chose the best of them for each rate. Thus, the code we are using is not necessarily optimally punctured and using an optimally punctured code we may achieve better performance results in simulations.

B. Results

1) Comparison of Bit Error Rates for Various Coding Schemes: In this section, we compare the bit error rates of the currently existing coding mechanisms with our proposed mechanisms, i.e. the case of independent parallel encoders and the case of using Hybrid Channel Codes. Note that for a system to be available, we set the maximum allowable value of the BER to 10^{-6}.

The results are shown in Fig. 9. Fig. 9(a) shows the simulation result for cases 1 and 2 and Figs. 9(b) and 9(c) show the results for cases 3, 4 and 5. First, note that we had to show the results in separate figures because the fixed rate FSO channel, as it is shown, requires about 44 dB of link margin to provide the desired bit error rates. In Figs. 9(a) and 9(b), we fixed the RF channel's SNR to 8 dB and 4.5 dB, respectively, and plotted the variations of BER with the FSO channel's SNR [1]. In Fig. 9(c), however, we fixed the SNR of the FSO channel to 4.5 dB and showed the variations of BER with the RF channel's SNR. This way, we can include the BER curves corresponding to different schemes in one figure. If we fix the SNR of the FSO or RF channel to other values, we will obtain similar figures in which the overall performance of the different systems is very similar to the figures we have shown. The energy per bit for each of the coding mechanisms is calculated as the weighted average of the energy per bit in the two channels. The weights used for averaging are the percents of time that each channel's transmitter is on. For each SNR, the BER is averaged over the attenuation probability density function.

We can see that using a back-up RF channel can cause a significantly better performance. However, the systems employing rate-adaptive codes lead to another 7 dB improvement over the system with fixed rate code. As in Fig. 9(b), Hybrid Channel Codes result in over two orders of magnitude improvement in BER over the other two systems using rate-adaptive codes. This is due to the media diversity and the effect of using non-uniform codes. In a system using independent parallel encoders with rate-adaptive coding, the two channels will be decoded separately and the output of the better channel can not help the decoding of the output of the worse channel. We also showed the result for the case of equal bandwidth RF and FSO channels. As you can see, there is a $0.5 - 0.7$ dB improvement in this case due to the longer code length and better error correction capability of the RF channel.

The capacity curve is also shown in the figure. We can see that although our code is being punctured over a broad range

[1]Note that to compare different systems, we need to draw 3D figures showing the BER versus the FSO and RF channel SNRs. However, the figures obtained in this way are not clear enough to be used for our comparison purposes.

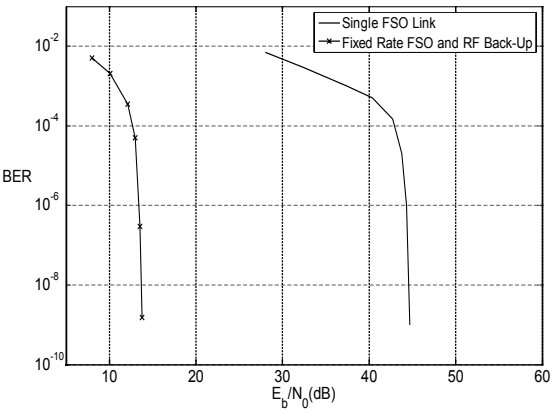

(a) BER performance of fixed rate single FSO link and fixed rate hybrid systems.

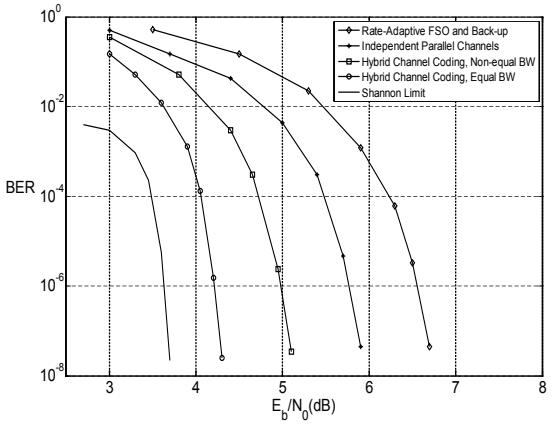

(b) BER performance of rate-adaptive systems and Hybrid Channel Coding when RF channel's SNR is fixed.

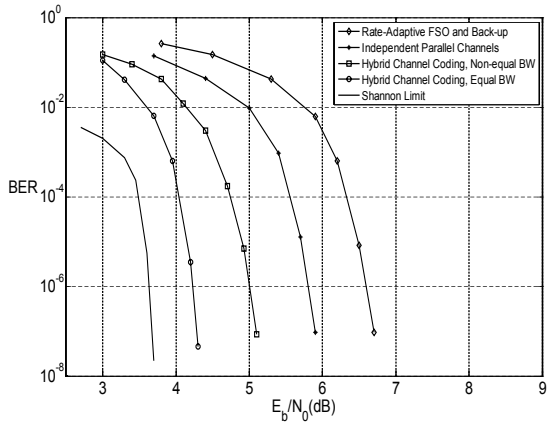

(c) BER performance of rate-adaptive systems and Hybrid Channel Coding when FSO channel's SNR is fixed.

Fig. 9. BER performance for different schemes.

of rates (from 0.15 to 0.9), we can still obtain good BERs and get to within 1.2 dB of the capacity in BER of 10^{-6}. We also observe that the penalty of keeping the second link always available is not too high when using Hybrid Channel Codes, another advantage along with the other benefits mentioned earlier.

2) Comparison of Throughput for Various Coding Schemes: In order to compare the throughput of different systems, we fixed the transmitted power for both transmitters and averaged, over the attenuation distribution, the throughput of different schemes in a long-time run. We collected the results in Table I for both equal and non-equal BW systems.

TABLE I
COMPARISON OF THE AVERAGE THROUGHPUT (IN GBPS) OBTAINED FOR DIFFERENT HYBRID SYSTEMS

System Type	Non-equal BW Channels	Equal BW Channels
Hybrid channel coding	1.02	1.841
Independent parallel encoders	0.957	1.585
Rate-adaptive FSO and RF back-up	0.916	1.543
Fixed rate FSO and RF back-up	0.763	1.25
Single FSO Link	0.559	0.559

TABLE II
THE TRADE-OFF BETWEEN AVAILABILITY AND THROUGHPUT FOR HYBRID CHANNEL CODES WITH DIFFERENT PARENT-CODE RATES

Rate of The Parent Code	Required Link Margin (dB)	Normalized Throughput
0.15	5	0.85
0.3	5.4	0.86
0.5	6.3	0.88

In the non-equal BW case, the fixed rate code over single FSO link can only achieve a throughput of 559 Mbps. However, the FSO/RF system with fixed rate back-up can achieve a throughput of 763 Mbps which is a considerable improvement over single FSO link. Hybrid Channel Coding achieves 1.02 Gbps while other rate-adaptive schemes can provide a throughput of about 916 and 957 Mbps each. Thus, Hybrid Channel Codes can achieve a 33% improvement over hybrid FSO/RF systems which are using a fixed rate code. In the equal BW case, our simulations show that Hybrid Channel Codes provide a throughput of 1.841 Gbps, i.e. 0.92 of the capacity. This is due to the superior performance of Hybrid Channel Codes in error correction when using equal BW channels. Note that in none of these systems we have data duplication over FSO and RF channels. If we were to compare Hybrid Channel Codes against a scheme with data duplication, we needed to consider the goodput instead of the throughput for a fair comparison.

3) Availability-Throughput Trade-off: In order to study the trade-off between availability and throughput, we consider the performance of Hybrid Channel Codes with different rates for the parent code. Table II shows the required link margin for availability and the achievable normalized throughput for different parent-code rates. We only consider our default system with unequal channel bandwidths. Note that using higher rates for the parent code leads to lower reliability although it results in a slight increase in the throughput. On the other hand, using parent codes with lower rates, we need to puncture more bits in good channel conditions which results in more decoding complexity.

V. Conclusion

One of the main issues in the design of hybrid FSO/RF communication systems is the difficulty of providing carrier class availability using these systems. In this paper, we suggest a novel hybrid FSO/RF technique that, unlike previous systems, utilizes both the FSO and RF channels effectively and increases system availability. The proposed novel system is a combination of media diversity mechanisms proposed earlier that utilizes novel codes to achieve the combined channel capacity of the FSO and the RF channels. We then design optimal codes, termed Hybrid Channel Codes, to achieve this combined channel capacity. These codes use non-uniform, rate-adaptive LDPC codes that in conjunction with the media diversity scheme can provide excellent performance improvements over the currently existing systems. Simulation results are provided to show that the new system proposed is better in terms of system availability, bit error rate performance and channel utilization (throughput and goodput). This paper provides a starting point for the implementation of a system that may solve some of the long standing issues of last-mile connectivity and disaster recovery. Future work can include the implementation of Hybrid Channel Codes using efficient VLSI architectures and a testbed to compare the performance of the proposed system to that of the existing systems.

References

[1] A. Mahdy and J. S. Deogun, "Wireless optical communications: a survey," in *Proc. IEEE Wireless Commun. Networking Conf. (WCNC)*, Mar. 2004, pp. 2399–2404.

[2] P. Clark and A. Sengers, "Wireless optical networking: challenges and solutions," in *Proc. IEEE MILCOM*, Oct. 2004, pp. 416–422.

[3] I. I. Kim, R. Ruigrok, and C. DeCusatis, "Wireless optical transmission of fast ethernet, FDDI, ATM, and ESCON protocol data using the terralink laser communication system," *SPIE J. Optical Engineering*, Dec. 1998.

[4] S. Muhammad, P. Kohldorfer, and E. Leitgeb, "Channel modeling for terrestrial free space optical links," in *Proc. IEEE ICTON*, July 2005, pp. 407–410.

[5] H. Wu, B. Hamzeh, and M. Kavehrad, "Achieving carrier class availability of FSO link via a complementary RF link," in *Proc. 38th Asilomar Conf. Signals, Systems Computers*, Nov. 2004, vol. 2, pp. 1483–1487.

[6] M. Gebhart, E. Leitgeb, and J. Bregenzer, "Atmospheric effects on optical wireless links," in *Proc. 7th International Conf. Telecommun., ConTEL*, Dec. 2003, pp. 395–399.

[7] Z. Jia, F. Ao, and Q. Zhu, "BER performance of the hybrid FSO/RF attenuation system," in *Proc. 7th International Symposium Antennas, Propagation EM Theory*, Oct. 2006, pp. 1–4.

[8] S. Bloom and W. Hartley, "The last-mile solution: hybrid FSO radio." white paper, AirFiber Inc., May 2002.

[9] K. Wakamori, K. Kazaura, and I. Oka, "Expriment on regional broadband network using free-space-optical communication systems," *J. Lightwave Technol.*, vol. 25, no. 11, pp. 3265–3273, 2007.

[10] V. Chan, "Coding for the turbulent atmospheric optical channel," *IEEE Trans. Commun.*, vol. 30, no. 1, pp. 269–275, 1982.

[11] Y. T. Koh and F. Davidson, "Interleaved concatenated coding for the turbulent atmospheric direct detection optical communication channel," *IEEE Trans. Commun.*, vol. 37, no. 6, pp. 648–651, 1989.

[12] J. Li and M. Uysal, "Error performance analysis of coded wireless optical links over atmospheric turbulence channels," in *Proc. IEEE Wireless Commun. Networking Conf. (WCNC)*, Mar. 2004.

[13] S. Navidpour, M. Uysal, and M. Kavehrad, "Performance bounds for correlated turbulent free-space optical channels," in *Proc. CERS*, Mar. 2006.

[14] X. Zhu and J. M. Kahn, "Performance bounds for coded free-space optical communications through atmospheric turbulence channels," *IEEE Trans. Commun.*, vol. 51, no. 8, pp. 1233–1239, 2003.

[15] J. Li and M. Uysal, "Achievable information rate for outdoor free space optical communication with intensity modulation and direct detection," in *Proc. IEEE GLOBECOM*, Nov. 2003, pp. 2654–2658.

[16] S. Trisno, I. Smolyaninov, S. Milner, and C. C. Davis, "Characterization of time delayed diversity to mitigate fading in atmospheric turbulence channels," *SPIE*, pp. 5892151–58921510, July 2005.

[17] E. Lee and V. Chan, "Part 1: optical communication over the clear turbulent atmospheric channel using diversity," *IEEE J. Sel. Areas Commun.*, vol. 22, no. 9, pp. 1896–1906, 2004.

[18] S. Z. Denic, I. Djordjevic, J. Anguita, B. Vasic, and M. A. Neifeld, "Information theoretic limits for free-space optical channels with and without memory," *IEEE J. Lightwave Technol.*, vol. 26, pp. 3376–3384, Oct 2008.

[19] N. Letzepis and A. G. Fabregas, "Outage probability of the MIMO Gaussian free-space optical channel with PPM," in *Proc. IEEE International Symposium Inf. Theory*, July 2008, pp. 2649–2653.

[20] S. M. Haas and J. H. Shapiro, "Capacity of wireless optical communications," *IEEE J. Sel. Areas Commun.*, vol. 21, no. 8, pp. 1346–1357, 2003.

[21] J. Akella, M. Yuksel, and S. Kalyanaraman, "Error analysis of multihop free-space optical communication," in *Proc. IEEE ICC*, May 2005, pp. 1777–1781.

[22] I. I. Kim and E. Korevaar, "Availability of free space optics (FSO) and hybrid FSO/RF systems," in *Proc. Optical Wireless Commun. IV*, Aug. 2001.

[23] L. B. Stotts, L. C. Andrews, P. C. Cherry, J. J. Foshee, P. J. Kolodzy, W. K. McIntire, R. L. P. Malcolm Northcott, H. A. Pike, B. Stadler, and D. W. Young, "Hybrid optical RF airborne communications," *Proc. IEEE*, vol. 97, pp. 1109–1127, June 2009.

[24] FreeSpaceOptics, Free space optics: informational website. [Online]. Available: http://www.freespaceoptic.com/

[25] K. Akhavan, M. Kavehrad, and S. Jivkova, "High-speed power-efficient indoor wireless infrared communication using code combining, part II," *IEEE Trans. Commun.*, vol. 50, pp. 1495–1502, Sep. 2002.

[26] H. Pishro-Nik, N. Rahnavard, and F. Fekri, "Non-uniform error correction using low-density parity-check codes," *IEEE Trans. Inf. Theory*, vol. 51, 2005.

[27] H. Pishro-Nik and F. Fekri, "Results on punctured low-density parity-check codes and improved iterative decoding techniques," *IEEE Trans. Inf. Theory*, vol. 53, pp. 599–614, 2007.

[28] H. Pishro-Nik and F. Fekri, "On raptor codes," in *Proc. IEEE ICC*, 2006.

[29] R. M. Tanner, "A recursive approach to low complexity codes," *IEEE Trans. Inf. Theory*, vol. 27, pp. 533–547, 1981.

[30] T. J.Richardson, M. A. Shokrollahi, and R. L. Urbanke, "Design of capacity-approaching irregular low-density parity-check codes," *IEEE Trans. Inf. Theory*, vol. 47, pp. 619–637, 2001.

[31] J. Ha, J. Kim, and S. W. McLaughlin, "Rate-compatible puncturing of low-density parity-check codes," *IEEE Trans. Inf. Theory*, vol. 50, pp. 2824–2836, 2004.

[32] D. J. C. MacKay, "Good error-correcting codes based on very sparse matrices," *IEEE Trans. Inf. Theory*, vol. 45, pp. 399–431, 1999.

[33] G. Miller and D. Burshtein, "Bounds on the maximum likelihood decoding error probability of low density parity check codes," *IEEE Trans. Inf. Theory*, vol. 47, pp. 2696–2710, 2001.

[34] C. Hsu and A. Anastasopoulos, "Capacity achieving LDPC codes through puncturing," in *Proc. International Conf. Wireless Networks, Commun. Mobile Computing*, 2005, pp. 1575–1580.

[35] E. A. Bucher, "Computer simulation of light pulse propagation for communication through thick clouds," *Appl. Opt.*, vol. 12, no. 10, pp. 2391–2400, 1973.

[36] B. Wu, B. Marchant, and M. Kavehrad, "Optical scattering in battlefield obscurants: analysis of channel spatial, angular and temporal dispersion," in *Proc. IEEE Military Commun. Conf. (MILCOM)*, 2007, pp. 1–6.

[37] B. Wu, Z. Hajjarian, and M. Kavehrad, "Free space optical communications through clouds: analysis of signal characteristics," *Appl. Opt.*, vol. 47, no. 17, pp. 3168–3176, 2008.

[38] R. Prasad, *OFDM for Wireless Communications Systems*. Artech House Publishers, 2004.

[39] S. Lee and M. Kavehrad, "Free-space optical communications with channel shortening filter and Viterbi equalizer," *International J. Wireless Inf. Networks*, vol. 16, no. 4, pp. 185–196, 2009.

[40] I. B. Djordjevic, B. Vasic, and M. A. Neifeld, "LDPC-coded OFDM for optical communication systems with direct detection," *IEEE J. Sel. Topics Quantum Electron.*, vol. 13, no. 5, pp. 1446–1454, 2007.

[41] I. I. Kim, B. McArthur, and E. J. Korevaar, "Comparison of laser beam propagation at 785 nm and 1550 nm in fog and haze for optical wireless communication," *SPIE Optical Wireless Commun. III*, vol. 4214, pp. 26–37, 2001.

[42] R. K. Crane, *Electromagnetic Wave Propagation Through Rain*. Wiley-Interscience, 1996.

[43] L. C. Andrews, R. L. Phillips, and C. Y. Hopen, *Laser Beam Scintillation with Applications*. Bellingham, WA: SPIE Press, 2001.
[44] M. Uysal, J. Li, and M. Yu, "Error rate performance analysis of coded free-space optical links over gamma-gamma atmospheric turbulence channels," *IEEE Trans. Wireless Commun.*, vol. 5, no. 6, pp. 1229–1233, 2006.
[45] P. Vasconcelos and L. Correia, "Fading characterization of the mobile radio channel at the millimetre waveband," in *Proc. IEEE Veh. Technol. Conf.*, May 1997, pp. 999–1003.
[46] J. Schöthier, "Wp3-study: the 60 GHz channel and its modelling," tech. report, IST-2001-32686 Broadway, 2001.
[47] G. M. Kizer, *Microwave Engineering*. Iowa State Press, 1990.
[48] NOAA, "National oceanic and atmospheric administration." [Online]. Available: http://www.nws.noaa.gov/
[49] S. Karp, R. M. Gigliardi, S. E. Moran, and L. B. Stotts, *Optical Channels*. Springer, 1988.

Ali Eslami received his B.Sc. and M.Sc. in electrical engineering from Sharif University of Technology, Tehran, Iran, in 2004 and 2006, respectively. He was a Research Assistant in the Information Systems and Security Lab (ISSL) in Sharif University from 2004 to 2007. He is currently pursuing a Ph.D. degree in electrical and computer engineering at the University of Massachusetts, Amherst. His research interests include error control coding, network information theory, and mathematical analysis of wireless networks.

Sarma Vangala holds master's degrees in electrical engineering and in computer science from the University of Massachusetts, Amherst, and from the University of South Florida, Tampa, respectively. His other topics of research include Transport Layer Protocols (in particular, TCP) and Internet security. He is currently working with Qualcomm Inc., San Diego, as a Senior Engineer. Recently he has been working on EvDO Rev B commercialization.

Hossein Pishro-Nik is an Assistant Professor of electrical and computer engineering at the University of Massachusetts, Amherst. He received a B.S. degree from Sharif University of Technology, and M.Sc. and Ph.D. degrees from Georgia Institute of Technology, all in electrical and computer engineering. His research interests include mathematical analysis of communication systems, in particular, error control coding, wireless networks, and vehicular ad hoc networks. His awards include an NSF Faculty Early Career Development (CAREER) award, an Outstanding Junior Faculty Award from UMass, and an Outstanding Graduate Research Award from Georgia Tech.